Tuning and amplifying the interactions in superconducting quantum circuits with subradiant qubits

Qi-Ming Chen [1,2,*], Fabian Kronowetter,[1,2] Florian Fesquet,[1,2] Kedar E. Honasoge,[1,2] Yuki Nojiri,[1,2] Michael Renger [1,2]
Kirill G. Fedorov,[1,2] Achim Marx [1] Frank Deppe,[1,2,3,†] and Rudolf Gross [1,2,3,‡]

[1]*Walther-Meißner-Institut, Bayerische Akademie der Wissenschaften, 85748 Garching, Germany*
[2]*Physik-Department, Technische Universität München, 85748 Garching, Germany*
[3]*Munich Center for Quantum Science and Technology (MCQST), Schellingstr. 4, 80799 Munich, Germany*

We propose a tunable coupler consisting of N fixed-frequency qubits, which can tune and even amplify the effective interaction between two superconducting quantum circuits. The tuning range of the interaction is proportional to N, with a minimum value of *zero* and a maximum that can exceed the physical coupling rates between the coupler and the circuits. The effective coupling rate is determined by the collective magnetic quantum number of the qubit ensemble, which takes only discrete values and is free from collective decay and decoherence. Using single-photon π-pulses, the coupling rate can be switched between arbitrary choices of the initial and final values within the dynamic range in a single step without going through intermediate values. A cascade of the couplers for amplifying small interactions or weak signals is also discussed. These results should not only stimulate interest in exploring the collective effects in quantum information processing, but also enable development of applications in tuning and amplifying the interactions in a general cavity-QED system.

I. INTRODUCTION

Tuning the coupling rate between two fixed-frequency superconducting quantum circuits, instead of tuning the characteristic frequency of each individual part, has attracted increasing interest in recent years as a promising way for scalable quantum computing [1–9]. The conventional method to realize such a tunable coupler is to place a Josephson junction, or SQUID, as a mediating element between the two circuits. From a circuit point of view, the junction can be regarded as a tunable positive inductance, which, together with other circuit elements such as capacitors or mutual inductors, can be used to form a tunable coupler [10–14]. Alternatively, one may also consider the junction as an off-resonant qubit which mediates the exchange of virtual photons between the two circuits [15–22]. A tunable coupling rate is achieved by adjusting the frequency detuning between the coupler qubit and the coupled circuits, while maintaining the former unexcited. This single-junction coupler has attracted great success in recent experiments. However, the dynamic range of the effective coupling rate is limited to the second order of the physical dispersive coupling rate. Moreover, the coupler can be very sensitive to experimental imperfections, including both systematic and stochastic errors in certain parameter regimes, because of the nonlinearity of the Josephson inductance.

Here we propose to use different steady states of one or several Josephson junctions to tune the coupling rate between two superconducting quantum circuits. The coupler is modeled by an ensemble of N homogeneous fixed-frequency and off-resonant qubits, also known as the Dicke model [23], and

is thus called the D-coupler. Instead of tuning the frequencies of the coupler qubits, a tunable interaction is achieved by preparing the qubits in different quantum states, corresponding to different collective angular and magnetic quantum numbers [16,18,24]. The dynamic range is proportional to the number of coupler qubits, where the maximum coupling rate may even exceed the individual coupling rates in the system for large N. On the other hand, the name, D-coupler, may also be interpreted as "decay- and decoherence-free" if we prepare the qubits in subradiant states [23]. It can also be understood as a digital coupler if we further restrict the subradiant states to be pairwise. In this case, the effective coupling rate takes only discrete values that are proportional to the total excitation number of the qubit ensemble [24]. Control of the coupling rate, between arbitrary initial and final choices within the dynamic range, can be realized in a single step with single-photon π-pulses [25]. In the meanwhile, the coupling rate needs not to go through any intermediate values during the tuning process. These properties make the D-coupler an ideal device in superconducting quantum circuits, despite the potential technical difficulty in sample design and fabrication, and should motivate more applications of the collective effects in quantum information processing [26–37].

II. THE DICKE COUPLER

We consider a system where the interaction between two circuits, X$_1$ and X$_2$, is mediated by an ensemble of N qubits, Q$_c$. The system Hamiltonian may be written as ($\hbar = 1$) [38]

$$H = \sum_{m=1}^{2} \sum_{n=1}^{N} \omega_m x_m^\dagger x_m + \frac{\omega_n}{2} \sigma_n^z + g_{m,n}(x_m^\dagger + x_m)\sigma_n^x$$
$$+ \sum_{(n,n')} g_{n,n'}(\sigma_n^+ \sigma_{n'}^- + \sigma_n^- \sigma_{n'}^+). \tag{1}$$

*qiming.chen@wmi.badw.de
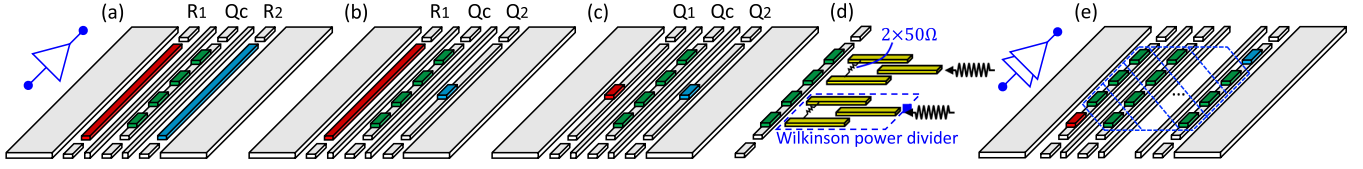†frank.deppe@wmi.badw.de
‡rudolf.gross@wmi.badw.de

FIG. 1. (a–c) Schematic of the D-coupler (green) between two resonators, R_1 and R_2, one resonator and one qubit, R_1 and Q_2, as well as two qubits, Q_1 and Q_2, which are colored in red and blue, respectively. The coupler is labeled as Q_c, which is an ensemble of N qubits. The effective coupling rate between the two circuits is determined by the collective magnetic quantum number, m, of Q_c. (d) A change of the magnetic quantum number, $m \rightarrow m'$, can be realized in a single step by applying $(m' - m)$ single photons to $(m' - m)$ Wilkinson power dividers, each of which couples to two qubits in the ensemble with a π phase difference. We note that the qubit number in the ensemble, N, is assumed to be *even*, while an *odd* N leads to a finite minimum coupling rate corresponding to the magnetic quantum numbers $\pm 1/2$. (e) A cascade of D layers of D-couplers (green) to mediate the interaction between two qubits colored in red and blue.

Here ω_m, x_m, and $x_m^\dagger$ are the resonant frequency, raising, and lowering operators of circuit X_m. Furthermore, ω_n and σ_n^α with $\alpha = x, y, z$ are the characteristic frequency and the standard Pauli operators of the nth coupler qubit, $g_{\alpha,\beta}$ is the physical coupling rate between the two parts α and β, and (n, n') takes all possible pairs in the ensemble. Depending on the commutation and anticommutation relations between x_m and $x_m^\dagger$, the above model can be used to describe a resonator-resonator (R-R) coupler $(x_1 \equiv r_1, x_2 \equiv r_2)$, a resonator-qubit (R-Q) coupler $(x_1 \equiv r_1, x_2 \equiv \sigma_2^-)$, or a qubit-qubit (Q-Q) coupler $(x_1 \equiv \sigma_1^-, x_2 \equiv \sigma_2^-)$, as schematically shown in Figs. 1(a)–1(c).

Assuming that the coupler qubits are largely detuned from the two circuits to be coupled, i.e., $g_{m,n} \ll \Delta_{m,n}, \Sigma_{m,n}$ where $\Delta_{m,n} = \omega_m - \omega_n$ and $\Sigma_{m,n} = \omega_m + \omega_n$, a dispersive approximation (DA) may be applied to Eq. (1) that diagonalizes the coupler degree of freedom to the second order of $g_{m,n}$. For simplicity and in the same spirit of the Dicke [23] or Tavis-Cummings model [39,40], we further assume the qubits to be homogeneous and use the collective angular momentum operators, $J^\alpha = \sum_{n=1}^N \sigma_n^\alpha$ with $\alpha = x, y, z$, to describe the whole ensemble [41]. Then the effective Hamiltonian can be written in a more compact form (see Appendix A for detailed derivation):

$$\tilde{H} = \sum_{m=1}^2 \omega_m x_m^\dagger x_m + \frac{1}{2}\left[\omega_c + \chi_m^-\left(x_m + x_m^\dagger\right)^2\right]J^z$$

$$- \sum_{m=1}^2 \frac{g_1 g_2}{2}\left(\frac{1}{\Delta_m} - \frac{1}{\Sigma_m}\right)J^z\left(x_1^\dagger + x_1\right)\left(x_2^\dagger + x_2\right)$$

$$+ \frac{g_c}{2}(J^+ J^- + J^- J^+) + \frac{\chi_m^+}{2}[\![x_m, x_m^\dagger]\!](J^x)^2, \quad (2)$$

where $\chi_m^\pm = -g_m^2(1/\Delta_m \pm 1/\Sigma_m)$, $g_m \equiv g_{m,n}$, $g_c \equiv g_{n,n'}$, and $[\![A, B]\!] = AB - BA$ is the commutation operator. One can verify that the angular quantum number, j, which is determined by $j(j+1) = \langle J^2 \rangle$, is a conserved quantity. However, the magnetic quantum number, m, which is an eigenvalue of $J^z/2$, may not be a good quantum number because of the counter-rotating term $(J^x)^2$. To be able to apply a rotating wave approximation (RWA), we further assume $\chi_m^+ \ll \omega_c$. Then J^z commutes with the Hamiltonian and can be replaced by its average during the time evolution if the system is initially prepared at its eigenstates. This results in an effective coupling

rate between X_1 and X_2,

$$g_{\mathrm{eff}} = -\sum_{m=1}^2 \frac{g_1 g_2}{2}\left(\frac{1}{\Delta_m} - \frac{1}{\Sigma_m}\right)\langle J^z \rangle. \quad (3)$$

The above result indicates that an arbitrary coupling rate, which corresponds to $-N \leqslant \langle J^z \rangle \leqslant N$, can be achieved by preparing the qubits in different collective states $|j, m\rangle$ with $j = 0, \ldots, N/2$, $m = -j, \ldots, j$. One may also prepare the coupler in an arbitrary superposition or mixture of the eigenstates $|j, m\rangle$, which results in a quantum effective coupling strength between the two circuits and may lead to novel applications. However, we restrict the coupler to be eigenstates in the rest of this paper. For a sufficiently large N, it is possible to achieve an effective coupling rate exceeding the physical rates between the coupler and either of the circuits, $g_{\alpha,\beta}$, while maintaining the requirements of DA and RWA. These properties show that a qubit ensemble described by the Dicke model can be used as a tunable coupler between two circuits and has a broad dynamic range proportional to the size of the ensemble.

We note that the frequencies of the two circuits being coupled are not necessarily the same, and the above discussions apply to a general system which can be described by the Dicke model. One may consider using the D-coupler as a transducer which converts a microwave photon to an optical photon and vice versa [15]. Here the qubit ensemble may be made of a thin layer of spin-1/2 materials, for example, a huge and homogeneous array of NV centers, at an intermediate frequency between microwave and optical frequencies. At the optimal condition

$$\frac{\omega_1 - \omega_2}{N} = g_2^2\left(\frac{1}{\Sigma_2} - \frac{1}{\Delta_2}\right) - g_1^2\left(\frac{1}{\Sigma_1} - \frac{1}{\Delta_1}\right), \quad (4)$$

where the two physically off-resonant modes are effectively on resonance such that a single photon can be perfectly transferred between them for a time duration of $t = (\pi + 2k\pi)/[g_1 g_2(1/\Delta_1 - 1/\Sigma_1 + 1/\Delta_2 - 1/\Sigma_2)N]$ for $k = 0, 1, \ldots$. This result may indicate a strong coupling rate between the microwave and optical modes for large N and, correspondingly, a high conversion efficiency ideally approaching unity.

For a qualitative estimation, we choose the frequency of the microwave and optical modes to be 2.744 GHz and 194.3 THz, respectively [42]. The coupler frequency is 2.87 GHz for an ensemble of NV centers, with a coupling
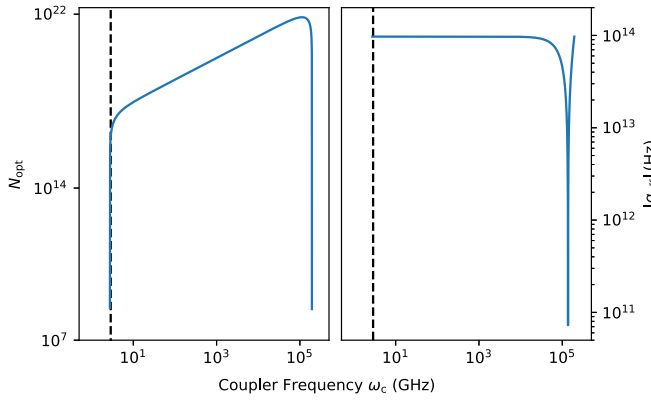
FIG. 2. The optimal number of qubits, N_{opt}, for microwave-optical photon conversion (left) and the absolute effective coupling rate, $|g_{\text{eff}}|$, between the microwave and optical modes (right). Here the coupler frequency, ω_c, is swept from the microwave to optical frequency. The dashed line indicates the frequency splitting between the spin-± 1 and the spin-0 states of an NV center in the electron ground state.

strength of 1 kHz between the coupler and either of the two modes. We estimate that the optimal condition leads to an effective coupling rate at the scale of 10^{14} Hz, which is in the deep strong coupling regime (Fig. 2 right). However, one should also note that the required number of homogeneous colored centers is approximately 2.4×10^{16}, which makes the optimal condition an extreme challenge to reach in real experiments (Fig. 2 left). In this regard, a practical implementation of the transducer requires a compromise between the effective coupling rate and the optimal condition. Alternatively, one may consider using two harmonic oscillators to form an effective spin-$N/2$ coupler, which is equivalent to an ensemble of N spin-1/2 qubits [43,44]. In either of the two cases, the collective effect of the Dicke model plays an important role in amplifying the weak interaction between the two off-resonant modes. A more detailed discussion of such a transducer relies on the specific parameters of the system and the compromises one may take, and is thus beyond the major interest of this study.

III. THE DECAY- AND DECOHERENCE-FREE COUPLER

The D-coupler is free from collective decay and decoherence if one restricts the collective states to a subspace spanned by subradiant states [23]. By definition, a subradiant state is an eigenstate of the collective angular momentum, $J^z/2$, with eigenvalue $m = -j$. In this regard, it is also an eigenstate of the collective lowering operator, J^-, with eigenvalue *zero*. In an open environment, the dynamics of the system may be described by the master equation with the Born-Markov approximation [45]

$$\dot{\rho} = -i[\![H, \rho]\!] + \frac{\gamma}{2}\mathcal{D}[J^-]\rho + \frac{\gamma_\phi}{2}\mathcal{D}[J^z]\rho, \qquad (5)$$

where γ and γ_ϕ are the energy relaxation and dephasing rates of the qubit ensemble, respectively, and $\mathcal{D}[J^\alpha]\rho = 2J^\alpha \rho (J^\alpha)^\dagger - (J^\alpha)^\dagger J^\alpha \rho - \rho (J^\alpha)^\dagger J^\alpha$ is the Lindblad superoperator. One can verify that the subradiant states are also

eigenstates of the Lindblad superoperator with eigenvalue *zero*. Thus, an arbitrary superposition of the subradiant states remains invariant during the dynamics of the open system with regard to collective decay and decoherence. Correspondingly, the effective coupling rate, which now takes only *zero* or negative eigenvalues of $\langle J^z \rangle$, is potentially stable in an open environment.

IV. THE DIGITAL COUPLER

Tuning of the coupling rate can be made ultrafast if we further restrict the subradiant states of the coupler to be pairwise, where each adjacent qubit pair $(2n, 2n + 1)$ takes only ground or singlet states, denoted as $|g\rangle = |0_{2n}0_{2n+1}\rangle$ and $|s\rangle = (|1_{2n}0_{2n+1}\rangle - |0_{2n}1_{2n+1}\rangle)\sqrt{2}$, respectively [25]. However, the dynamic range of the effective coupling strength is not affected because of the degeneracy of the subradiant states. This restriction also relaxes the original assumption of a collective decay and decoherence for all the coupler qubits into that for each qubit pair $(2n, 2n + 1)$ [24]. The coupling rate is controlled digitally by counting the total number of excitations in the qubit ensemble. Different from our earlier proposal for controlling the R-R coupling rate [24], we describe an alternative method that applies to a general system and results into an even faster switch of g_{eff} with beam splitters and single-photon sources [25].

As schematically shown in Fig. 1(d), the control protocol may consist of a Wilkinson power divider, which is modeled as a beam splitter routing an incident single microwave photon to two different paths simultaneously but with a π-phase difference [46–49]. At the end of each path, we couple one qubit to it and describe the photon-qubit interaction by a Jaynes-Cummings model [50]. Assuming that the two addressed qubits are initially in the ground state, $|g\rangle$, the single-photon drive increases the magnetic quantum number, m, by one and results in a singlet state $|s\rangle$ [25]. Alternatively, if the qubits are initially in the singlet state, they will end up in the ground state with $m \to (m - 1)$ [25]. For an ensemble of $N/2$ qubit pairs, one can apply $N/2$ single-photon π-pulses to them in parallel, and switch the coupling from an arbitrary initial to the final value in a single step. Interestingly, the coupling rate need not to go through any intermediate values during the tuning process if the skew among different beam splitters is negligibly small.

V. CASCADE OF D-COUPLERS

The D-coupler may also be cascaded in a chain with several layers of qubit ensembles, as schematically shown in Fig. 1(e). To simplify our discussion, we consider a system with D layers of N homogeneous qubits, where every two adjacent layers are coupled by an XY-type interaction:

$$\begin{aligned} H = &\sum_{m=1}^{2} \omega_m x_m^\dagger x_m + \sum_{d=1}^{D} \frac{\omega_c}{2} J_d^z \\ &+ g_1 (x_1^\dagger + x_1) J_1^x + g_2 (x_2^\dagger + x_2) J_D^x \\ &+ \sum_{d=1}^{D-1} g_c (J_d^+ J_{d+1}^- + J_d^- J_{d+1}^+). \end{aligned} \qquad (6)$$
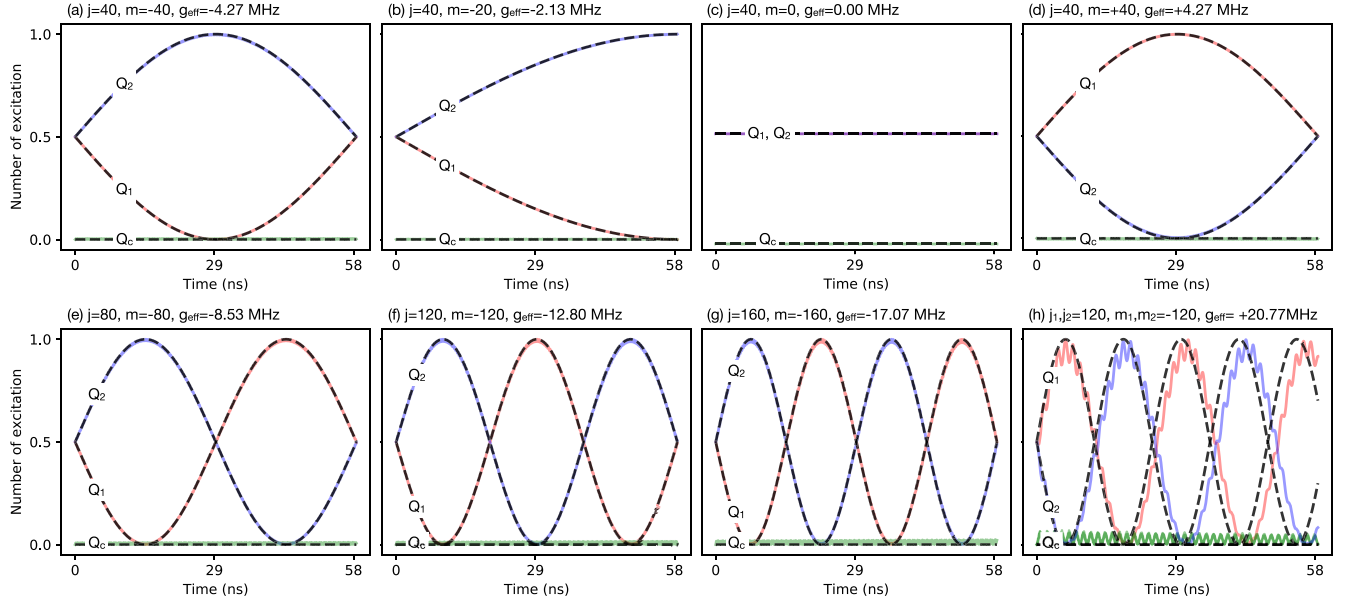
FIG. 3. (a–d) When operating a 80-qubit coupler with different magnetic quantum numbers, m, the two qubits under coupled exchange photons with different Rabi frequency. The interaction can be turned off when $m = 0$, while the maximum coupling rate, ± 4.27 MHz, is achieved when $m = \pm 40$. (e–g) Keeping the parameters unchanged while increasing the number of coupler qubits from 160 to 320, the effective coupling rate increases linearly from -8.53 MHz through -12.80 MHz to -17.07 MHz. In the last case, $|g_{\mathrm{eff}}|$ is 1.7 times larger than the physical coupling rate between a single qubit and the coupler. (h) Dynamics of the system with a cascade of two couplers, where each layer contains 240 homogeneous qubits. In all panels, the red and blue curves correspond to the population of the two qubits under coupled, and green curves the magnetic quantum number of the qubit ensemble deviating from m. They are the simulation result with the original Hamiltonians, Eqs. (1) and (6), while the dashed curves correspond to the predictions of the effective Hamiltonians.

We focus on the case where all the qubits are initially prepared in the ground state, corresponding to the maximum effective coupling rate between X_1 and X_2. For large N, the collective qubits may be approximately described by a giant quantum oscillator with $J_d^+ \approx \sqrt{N} a_d^\dagger$, $J_d^- \approx \sqrt{N} a_d$, and $J_d^z = 2 a_d^\dagger a_d - N$ [51–55].

Similar to the definition of magnons in a XY spin chain [56–59], we diagonalize the coupler part of the Hamiltonian by introducing a collective operator

$$a_k^\pm = \sqrt{\frac{2}{D+1}} \sum_{d=1}^{D} \sin\left(\frac{dk\pi}{D+1}\right) a_d^\pm, \text{ for } k = 1, \ldots, D. \quad (7)$$

We are interested in the parameter regime where all the "magnons" are largely off-resonant to the two circuits, i.e., $g_{m,k} \ll \Delta_{m,k}, \Sigma_{m,k}$ where $g_{m,k} = \sqrt{N} g_m \sin[mk\pi/(D+1)] \sqrt{2/(D+1)}$ is the coupling rate between X_m and the magnon-like mode, a_k, at frequency $\omega_k = \omega_c + 2 g_c N \cos[k\pi/(D+1)]$. Then we apply a dispersive approximation (DA) to transform the component-coupler interactions into an effective interaction between X_1 and X_2. The effective Hamiltonian is too complicated to display here (see Appendix B for detail), while the effective coupling rate is similar to the single-layer case:

$$g_{\mathrm{eff}} = \frac{N g_1 g_2}{D+1} \sum_{m=1}^{2} \sum_{k=1}^{D} \sin\left(\frac{mk\pi}{D+1}\right) \left(\frac{1}{\Delta_{m,k}} - \frac{1}{\Sigma_{m,k}}\right). \quad (8)$$

Surprisingly, g_{eff} is almost independent of the number of layers, D. For a relatively small qubit number, N, in each layer, i.e., $N g_c \ll \Delta_{m,k}, \Sigma_{m,k}$, the value of g_{eff} scales quadratically with N. With the increase of N, the exponent of the power law increases monotonically until DA breaks down. In this case, one may enlarge the detuning frequency and add more layers and qubits at the same time to achieve a balance between the amplification rate and the validity of the effective model. However, we should note that an Ising-type interaction between two adjacent layers causes a correction in Eq. (8), as revealed in Appendix B, which may lead to a larger g_{eff} in certain parameter regimes. Besides, a varying-frequency design of the coupler qubits among different layers may also lead to a different expression of g_{eff}.

VI. SIMULATION RESULTS

For illustration, we simulate the dynamics of a system which consists of two qubits and a D-coupler with 80 qubits, as shown in Figs. 3(a)–3(d). The two qubits are resonant at 1 GHz and largely detuned from the coupler qubits that are fixed at 4 GHz. The physical coupling rate, g_m, is set as $+10$ MHz, which fulfills the requirements of both DA and RWA. The possibly small qubit crosstalk inside the coupler is neglected for simplicity. From Fig. 3(a) to Fig. 3(d), we control the effective coupling rate, from -4.27 MHz to $+4.27$ MHz, by engineering the qubit ensemble in different collective states. The coupling is completely turned off in Fig. 3(c), when the magnetic quantum number is *zero*. It

also changes the sign comparing Figs. 3(a) and 3(d), which corresponds to the different signs of the magnetic quantum numbers.

Next, we keep all the coupler qubits in the ground state and increase the qubit number to 160, 240, and 320, as shown in Figs. 3(e)–3(g). Correspondingly, the effective coupling rate increases linearly from -8.53 through -12.80 to -17.07 MHz. Here the maximum value of g_{eff} is 1.7 times larger than the physical coupling rate, g_m, while the effective Hamiltonian, Eq. (2), still faithfully describes the dynamics of the system. This observation clearly demonstrates that an amplification of the interactions can be achieved in superconducting quantum circuits, which has not yet been reported in the literature. However, one may also note a small and periodic excitation of the coupler for increasingly large N, which is mainly caused by the finite ratio of g_m/Δ_m that limits the accuracy of the DA. These ripples can be effectively suppressed by increasing the detuning frequency and the qubit number by the same scaling factor, while keeping the effective coupling rate unchanged.

In Fig. 3(h) we simulate the system dynamics with a two-layer coupler, where each layer contains 240 collective qubits. The coupling rate between two adjacent layers, g_c, is assumed to be $+10$ MHz, while the other parameters are set identical to Figs. 3(a)–3(g). Regardless of the noticeable ripples in the excitation numbers, we obtain an effective coupling rate of around $+20.77$ MHz, which is much larger than that for the single-layer case shown in Fig. 3(f). The sign of the coupling rate is also different from Fig. 3(f). However, considering the total number of 480 qubits in the two-layer coupler, adding more layers may not amplify the interactions as efficiently as increasing the number of qubits in a single layer, which is estimated to be -25.60 MHz for the same number of qubits. Moreover, the amplification rate may even decrease when adding an addition layer in certain scenarios. For example, we obtain an effective coupling rate of $+5.12$ MHz for two layers of 160 qubits, while it is -8.53 MHz for a single layer of 160 qubits, as shown in Fig. 3(e).

Finally, we numerically study how the effective qubit-qubit interaction may be influenced by introducing a small inhomogeneity among the coupler qubits, as shown in Fig. 4. Although the natural qubits, for example, spins, are intrinsically homogeneous, it is a technical challenge to fabricate an ensemble of superconducting qubits with identical properties. This task is even more difficult if the qubits are assumed to be fixed frequency, where a fine tuning of the qubit frequencies is not allowed after fabrication. Here we randomly sample each individual single-qubit parameter, ω_n and $g_{m,n}$ in Eq. (1), within a range spanned by up to $\pm 1.5\%$ of their design values. With the increase of qubit inhomogeneity, the transition curve deviates increasingly from the exact result. This deviation depends also on the magnetic quantum number, m, of the coupler qubits. However, the effective interaction remains approximately in the same form of Eq. (3) despite a small shift of the Rabi frequency. This observation demonstrates the robustness of the proposed D-coupler, while the effective coupling rate, g_{eff}, must be calibrated in experiments in the presence of a small qubit inhomogeneity.
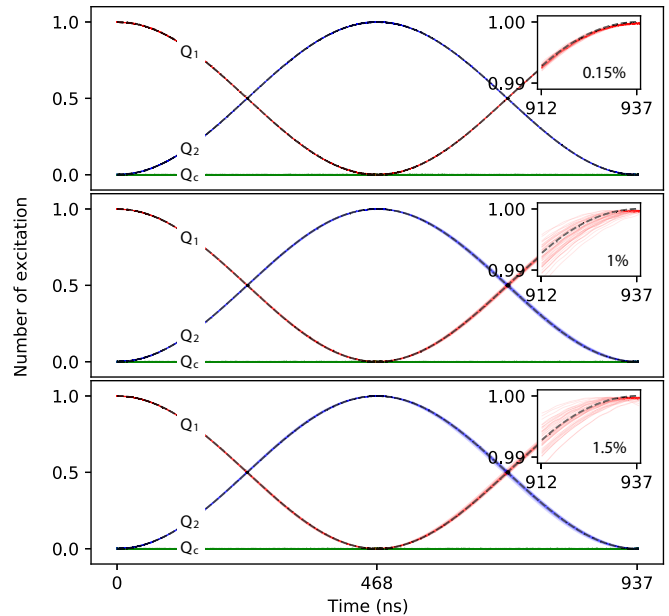

FIG. 4. The photon number transition between two qubits, which is mediated by a 10-qubit coupler. From top to the bottom, we perturb the parameters of each single coupler qubit, ω_n and $g_{m,n}$, by $\pm 0.15\%$, $\pm 1\%$, and $\pm 1.5\%$ of their ideal values, which follows a uniform distribution in the given range. The other simulation parameters are set identical to that in Fig. 3. In all the panels, the red and blue curves correspond to the population of the two effectively coupled qubits, which are initially prepared in the excited and ground states, respectively. The green curves correspond to the magnetic quantum number of the qubit ensemble deviating from $m = -5$, where the coupler qubits are initially in the ground state. The dashed curves correspond to the ideal Rabi oscillation. The simulation is repeated for 50 times, and the inset shows the results in a smaller range.

VII. CONCLUSIONS AND OUTLOOK

We have proposed a so-called D-coupler based on the Dicke model, and showed that it can be used to tune and amplify the effective interactions between two general circuits. The effective coupling rate is controlled by the collective magnetic quantum number of the qubit ensemble, and it is free from collective decay and decoherence when the qubits are prepared in the subradiant states. The tuning procedure, from any initial to final values, is achieved in a single step by applying single-photon π-pulses, without going through any intermediate values. The dynamic range scales linearly with the number of qubits, where the maximum can be made larger than the physical coupling rates between the coupler and the circuits.

We have also discussed a multilayer design of the D-coupler. The circuit configuration is reminiscent to a traveling wave parametric amplifier (TWPA), which may be seen as a *series* configuration of the coupler qubits. In this perspective, amplification from the input to output fields may happen in the presence of a parametric driving field, when the effective coupling rate between the end qubits exceeds a threshold relating to their external decay rates [60]. However, our result indicates that a *parallel* configuration of the coupler qubits may be an alternative and more efficient way to

achieve quantum limited amplification at the same number of junctions.

Despite the collective properties, one major difference between the D-coupler and most of the existing proposals is that the effective coupling rate is controlled by the quantum state of the coupler but not the detuning frequency. Hence, the coupler can be made of only one or two fixed-frequency qubits, which significantly simplifies the sample fabrication and, most importantly, leads to a flux-free design of superconducting quantum circuits where the qubit properties can be optimized with regard to only one noise source, i.e., the charge noise. One may also consider engineering the coupler state in the steady states of a driven-dissipative setup, which relaxes the assumption of a collective reservoir and may result into a more robust implementation. An experimental realization of

our protocol could offer significant advantages in designing superconducting quantum circuits for quantum information processing.

APPENDIX A: EFFECTIVE HAMILTONIAN WITH ONE LAYER

We consider a system, $H = H_0 + V$, where two general circuit components are coupled via a qubit ensemble

$$H_0 = \sum_{m=1}^{2} \omega_m x_m^\dagger x_m + \sum_{n=1}^{N} \frac{\omega_n}{2} \sigma_n^z + \sum_{\{n,n'\}} g_{n,n'} (\sigma_n^+ \sigma_{n'}^- + \sigma_n^- \sigma_{n'}^+), \tag{A1}$$

$$V = \sum_{m=1}^{2} \sum_{n=1}^{N} \underbrace{g_{m,n} (x_m^\dagger \sigma_n^- + x_m \sigma_n^+)}_{V_1} + \underbrace{g_{m,n} (x_m^\dagger \sigma_n^+ + x_m \sigma_n^-)}_{V_2}. \tag{A2}$$

Here ω_m, x_m, and $x_m^\dagger$ are the resonant frequency, raising, and lowering operators, respectively, of the mth system component $\mathrm{X_m}$. Furthermore, ω_n and σ_n^α with $\alpha = x, y, z$ are the characteristic frequency and standard Pauli operators of the nth qubit in the ensemble with a total qubit number of N, $g_{\alpha,\beta}$ is the coupling rate between the two components α and β, and $\{n, n'\}$ takes all possible pairs in the ensemble. To transform the component-coupler interaction into an effective component-component interaction to the second order of $g_{\alpha,\beta}$, we apply the following unitary transformation to the original Hamiltonian [64]:

$$U = \exp\left[\overbrace{\sum_{m=1}^{2} \sum_{n=1}^{N} -\frac{g_{m,n}}{\Delta_{m,n}} (x_m^\dagger \sigma_n^- - x_m \sigma_n^+)}^{X_1} + \overbrace{\sum_{m=1}^{2} \sum_{n=1}^{N} -\frac{g_{m,n}}{\Sigma_{m,n}} (x_m^\dagger \sigma_n^+ - x_m \sigma_n^-)}^{X_2} \right]. \tag{A3}$$

On the one hand, we have $[\![H_0, X_1 + X_2]\!] = -V$. The transformation can be simplified as $U^\dagger H U = H_0 + (1/2)[\![V, X_1 + X_2]\!]$ to the second-order accuracy of $g_{m,n}/\Delta_{m,n}$ and $g_{m,n}/\Sigma_{m,n}$. On the other hand, we have

$$[\![V_1, X_1]\!] = -\frac{g_{m,n}}{\Delta_{m,n}} \big\{ g_{m',n} \sigma_n^z (x_1^\dagger x_2 + x_1^\dagger x_2) + g_{m,n} (\sigma_n^z \{x_m, x_m^\dagger\} + [\![x_m, x_m^\dagger]\!]) + g_{m,n'} [\![x_m, x_m^\dagger]\!] (\sigma_n^+ \sigma_{n'}^- + \sigma_n^- \sigma_{n'}^+) \big\}, \tag{A4}$$

$$[\![V_1, X_2]\!] = \frac{g_{m,n}}{\Sigma_{m,n}} \big\{ g_{m',n} \sigma_n^z (x_1^\dagger x_2^\dagger + x_1 x_2) + g_{m,n} \sigma_n^z (x_m^{\dagger 2} + x_m^2) - g_{m,n'} [\![x_m, x_m^\dagger]\!] (\sigma_n^+ \sigma_{n'}^+ + \sigma_n^- \sigma_{n'}^-) \big\}, \tag{A5}$$

$$[\![V_2, X_1]\!] = -\frac{g_{m,n}}{\Delta_{m,n}} \big\{ g_{m',n} \sigma_n^z (x_1^\dagger x_2^\dagger + x_1 x_2) + g_{m,n} \sigma_n^z (x_m^{\dagger 2} + x_m^2) + g_{m,n'} [\![x_m, x_m^\dagger]\!] (\sigma_n^+ \sigma_{n'}^+ + \sigma_n^- \sigma_{n'}^-) \big\}, \tag{A6}$$

$$[\![V_2, X_2]\!] = \frac{g_{m,n}}{\Sigma_{m,n}} \big\{ g_{m',n} \sigma_n^z (x_1^\dagger x_2 + x_1^\dagger x_2) + g_{m,n} (\sigma_n^z \{x_m, x_m^\dagger\} - [\![x_m, x_m^\dagger]\!]) - g_{m,n'} [\![x_m, x_m^\dagger]\!] (\sigma_n^+ \sigma_{n'}^- + \sigma_n^- \sigma_{n'}^+) \big\}. \tag{A7}$$

Here we have omitted the summation symbols over m and n for simplicity of notation; m' and n' indicate all the different numbers from m and n. In total, we obtain the effective Hamiltonian

$$\begin{aligned}
\tilde{H} &= \omega_m x_m^\dagger x_m + \frac{\omega_n}{2} \sigma_n^z + \frac{g_{n,n'}}{2} \sigma_n^x \sigma_{n'}^x + \frac{g_{m,n} g_{m',n}}{2} \left(\frac{1}{\Sigma_{m,n}} - \frac{1}{\Delta_{m,n}} \right) \sigma_n^z (r_1^\dagger + r_1)(r_2^\dagger + r_2) \\
&\quad + \frac{g_{m,n}^2}{2} \left(\frac{1}{\Sigma_{m,n}} - \frac{1}{\Delta_{m,n}} \right) \sigma_n^z (x_1 + x_1^\dagger)^2 - \frac{g_{m,n}^2}{2} \left(\frac{1}{\Sigma_{m,n}} + \frac{1}{\Delta_{m,n}} \right) [\![x_m, x_m^\dagger]\!] (\sigma_n^- + \sigma_n^+)^2 \\
&\quad - \frac{g_{m,n} g_{m,n'}}{2} \left(\frac{1}{\Sigma_{m,n}} + \frac{1}{\Delta_{m,n}} \right) [\![x_m, x_m^\dagger]\!] \sigma_n^x \sigma_{n'}^x.
\end{aligned} \tag{A8}$$

For the cases with two resonators, one resonator and one qubit, and two qubits, respectively, we have the following effective Hamiltonians:

$$\tilde{H}_{\text{R-R}} = \sum_{m=1}^{2} \sum_{n=1}^{N} \left[\omega_m + g_{m,n}^2 \left(\frac{1}{\Sigma_{m,n}} - \frac{1}{\Delta_{m,n}} \right) \sigma_n^z \right] r_m^\dagger r_m + \frac{g_{1,n} g_{2,n}}{2} \left(\frac{1}{\Sigma_{m,n}} - \frac{1}{\Delta_{m,n}} \right) \sigma_n^z (r_1^\dagger + r_1)(r_2^\dagger + r_2)$$

$$+ \frac{1}{2} \left[\omega_n + g_{m,n}^2 \left(\frac{1}{\Sigma_{m,n}} - \frac{1}{\Delta_{m,n}} \right) (r_m^\dagger r_m^\dagger + r_m r_m + 1) \right] \sigma_n^z$$

$$+ \sum_{n=1}^{N} \sum_{n' \neq n} \frac{1}{2} \left[g_{n,n'} - g_{m,n} g_{m,n'} \left(\frac{1}{\Sigma_{m,n}} + \frac{1}{\Delta_{m,n}} \right) \right] \sigma_n^x \sigma_{n'}^x, \tag{A9}$$

$$\tilde{H}_{\text{R-Q}} = \sum_{m=1}^{2} \sum_{n=1}^{N} \left[\omega_1 + g_{1,n}^2 \left(\frac{1}{\Sigma_{1,n}} - \frac{1}{\Delta_{1,n}} \right) \sigma_n^z \right] r_1^\dagger r_1 + \left[\omega_2 + g_{2,n}^2 \left(\frac{1}{\Sigma_{2,n}} + \frac{1}{\Delta_{2,n}} \right) \right] \frac{\sigma_2^z}{2}$$

$$+ \frac{g_{1,n} g_{2,n}}{2} \left(\frac{1}{\Sigma_{m,n}} - \frac{1}{\Delta_{m,n}} \right) \sigma_n^z (r_1^\dagger + r_1) \sigma_2^x$$

$$+ \frac{1}{2} \left[\omega_n + g_{1,n}^2 \left(\frac{1}{\Sigma_{1,n}} - \frac{1}{\Delta_{1,n}} \right) (r_1^\dagger r_1^\dagger + r_1 r_1 + 1) + g_{2,n}^2 \left(\frac{1}{\Sigma_{2,n}} - \frac{1}{\Delta_{2,n}} \right) \right] \sigma_n^z$$

$$+ \sum_{n=1}^{N} \sum_{n' \neq n} \frac{1}{2} \left[g_{n,n'} - g_{1,n} g_{1,n'} \left(\frac{1}{\Sigma_{1,n}} + \frac{1}{\Delta_{1,n}} \right) + g_{2,n} g_{2,n'} \left(\frac{1}{\Sigma_{2,n}} + \frac{1}{\Delta_{2,n}} \right) \sigma_2^z \right] \sigma_n^x \sigma_{n'}^x, \tag{A10}$$

$$\tilde{H}_{\text{Q-Q}} = \sum_{m=1}^{2} \sum_{n=1}^{N} \left[\omega_m + g_{m,n}^2 \left(\frac{1}{\Sigma_{m,n}} + \frac{1}{\Delta_{m,n}} \right) \right] \frac{\sigma_m^z}{2} + \frac{g_{1,n} g_{2,n}}{2} \left(\frac{1}{\Sigma_{m,n}} - \frac{1}{\Delta_{m,n}} \right) \sigma_n^z \sigma_1^x \sigma_2^x$$

$$+ \frac{1}{2} \left[\omega_n + g_{m,n}^2 \left(\frac{1}{\Sigma_{m,n}} - \frac{1}{\Delta_{m,n}} \right) \right] \sigma_n^z + \sum_{n=1}^{N} \sum_{n' \neq n} \frac{1}{2} \left[g_{n,n'} + g_{m,n} g_{m,n'} \left(\frac{1}{\Sigma_{m,n}} + \frac{1}{\Delta_{m,n}} \right) \sigma_m^z \right] \sigma_n^x \sigma_{n'}^x. \tag{A11}$$

If we further assume the homogeneity among the coupler qubits, we use the collective angular momentum operators to describe the whole qubit ensemble and arrive at a more compact form of the effective Hamiltonian. They are

$$\tilde{H}_{\text{R-R}} = \sum_{m=1}^{2} \left[\omega_m + g_m^2 \left(\frac{1}{\Sigma_m} - \frac{1}{\Delta_m} \right) J^z \right] r_m^\dagger r_m + \frac{g_1 g_2}{2} \left(\frac{1}{\Sigma_m} - \frac{1}{\Delta_m} \right) J^z (r_1^\dagger + r_1)(r_2^\dagger + r_2)$$

$$+ \frac{1}{2} \left[\omega_{\text{c}} + g_m^2 \left(\frac{1}{\Sigma_m} - \frac{1}{\Delta_m} \right) (r_m^\dagger r_m^\dagger + r_m r_m + 1) \right] J^z + \frac{1}{2} \left[g_{\text{c}} - g_m^2 \left(\frac{1}{\Sigma_m} + \frac{1}{\Delta_m} \right) \right] (J^x)^2, \tag{A12}$$

$$\tilde{H}_{\text{R-Q}} = \sum_{m=1}^{2} \left[\omega_1 + g_1^2 \left(\frac{1}{\Sigma_1} - \frac{1}{\Delta_1} \right) J^z \right] r_1^\dagger r_1 + \left[\omega_2 + g_2^2 \left(\frac{1}{\Sigma_2} + \frac{1}{\Delta_2} \right) (J^x)^2 \right] \frac{\sigma_2^z}{2} + \frac{g_1 g_2}{2} \left(\frac{1}{\Sigma_m} - \frac{1}{\Delta_m} \right) J^z (r_1^\dagger + r_1) \sigma_2^x$$

$$+ \frac{1}{2} \left[\omega_{\text{c}} + g_1^2 \left(\frac{1}{\Sigma_1} - \frac{1}{\Delta_1} \right) (r_1^\dagger r_1^\dagger + r_1 r_1 + 1) + g_2^2 \left(\frac{1}{\Sigma_2} - \frac{1}{\Delta_2} \right) \right] J^z$$

$$+ \frac{1}{2} \left[g_{\text{c}} - g_1^2 \left(\frac{1}{\Sigma_1} + \frac{1}{\Delta_1} \right) \right] (J^x)^2, \tag{A13}$$

$$\tilde{H}_{\text{Q-Q}} = \sum_{m=1}^{2} \left[\omega_m + g_m^2 \left(\frac{1}{\Sigma_m} + \frac{1}{\Delta_m} \right) (J^x)^2 \right] \frac{\sigma_m^z}{2} + \frac{g_1 g_2}{2} \left(\frac{1}{\Sigma_m} - \frac{1}{\Delta_m} \right) J^z \sigma_1^x \sigma_2^x$$

$$+ \frac{1}{2} \left[\omega_{\text{c}} + g_m^2 \left(\frac{1}{\Sigma_m} - \frac{1}{\Delta_m} \right) \right] J^z + \frac{1}{2} g_{\text{c}} (J^x)^2. \tag{A14}$$

APPENDIX B: EFFECTIVE HAMILTONIAN WITH MULTIPLE LAYERS

We consider a system with D layers of N homogeneous qubits, where any two adjacent layers are coupled by an XY-type interaction

$$H = \sum_{m=1}^{2} \omega_m x_m^\dagger x_m + \sum_{d=1}^{D} \frac{\omega_{\text{c}}}{2} J_d^z + \sum_{d=1}^{D-1} g_{\text{c}} (J_d^+ J_{d+1}^- + J_d^- J_{d+1}^+) + g_1 (x_1^\dagger + x_1) J_1^x + g_2 (x_2^\dagger + x_2) J_d^x. \tag{B1}$$

By assuming that $\langle J_d^z \rangle \approx -N/2$, we introduce the following replacement of variables for large N [51–55]:

$$J_d^+ \approx \sqrt{N}a_d^\dagger, \; J_d^- \approx \sqrt{N}a_d, \; J_d^z = 2a_d^\dagger a_d - N. \tag{B2}$$

This gives

$$H = \sum_{m=1}^{2} \omega_m x_m^\dagger x_m + \sqrt{N}g_1(x_1^\dagger + x_1)(a_1^\dagger + a_1) + \sqrt{N}g_2(x_2^\dagger + x_2)(a_d^\dagger + a_d)$$

$$+ \sum_{d=1}^{D} \omega_c a_d^\dagger a_d + \sum_{d=1}^{D-1} Ng_c\big(a_d^\dagger a_{d+1} + a_d a_{d+1}^\dagger\big). \tag{B3}$$

We note that the last term should be written as $\sum_{d=1}^{D-1} Ng_c(a_d^\dagger + a_d)(a_{d+1}^\dagger + a_{d+1})$ for an Ising-type interaction, described by $g_c J_d^x J_{d+1}^x$, between two adjacent layers.

Similar to the definition of magnons in a XY-type spin chain [56–59], we define

$$a_k^\pm = \sqrt{\frac{2}{D+1}} \sum_{d=1}^{D} \sin\left(\frac{sk\pi}{D+1}\right)a_d^\pm. \tag{B4}$$

The Hamiltonian can be written as

$$H_0 = \sum_{m=1}^{2} \omega_m x_m^\dagger x_m + \sum_{k=1}^{D} (\omega_c + 2g_k)a_k^\dagger a_k, \tag{B5}$$

$$V = \sum_{m=1}^{2}\sum_{k=1}^{N} \underbrace{g_{m,k}\big(x_m^\dagger a_k + x_m a_k^\dagger\big)}_{V_1} + \underbrace{g_{m,k}\big(x_m^\dagger a_k^\dagger + x_m a_k\big)}_{V_2}, \tag{B6}$$

where $g_k = Ng_c \cos[k\pi/(D+1)]$, $g_{m,k} = \sqrt{N}g_m \sin[mk\pi/(D+1)]\sqrt{2/(D+1)}$. For an Ising-type interaction, one may add $\sum_{k=1}^{D} g_k(a_k^{\dagger 2} + a_k^2)$ in H_0.

To derive the effective Hamiltonian, we apply the following unitary transformation:

$$U = \exp\left[\overbrace{\sum_{m=1}^{2}\sum_{k=1}^{D} \lambda_{m,k}^-(x_m^\dagger a_k - x_m a_k^\dagger)}^{X_1} + \overbrace{\sum_{m=1}^{2}\sum_{k=1}^{D} \lambda_{m,k}^+(x_m^\dagger a_k^\dagger - x_m a_k)}^{X_2}\right]. \tag{B7}$$

We obtain

$$[\![H_0, X_1 + X_2]\!] = \lambda_{m,k}^-(\Delta_{m,n} - 2g_k)(x_m^+ a_k + x_m^- a_k^\dagger) + \lambda_{m,k}^+(\Sigma_{m,n} + 2g_k)(x_m^+ a_k^\dagger + x_m^- a_k), \tag{B8}$$

$$[\![H_0, X_1 + X_2]\!] = [\lambda_{m,k}^-\Delta_{m,n} + 2(\lambda_{m,k}^+ - \lambda_{m,k}^-)g_k](x_m^+ a_k + x_m^- a_k^\dagger) + [\lambda_{m,k}^+\Sigma_{m,n} + 2(\lambda_{m,k}^+ - \lambda_{m,k}^-)g_k](x_m^+ a_k^\dagger + x_m^- a_k), \tag{B9}$$

for the XY- and Ising-type interactions, respectively. The rest of the commutators are

$$[\![V_1, X_1]\!] = -\lambda_{m,k}^-\big\{g_{m',k}(x_1^\dagger x_2 + x_1 x_2^\dagger) + g_{m,k}\{x_m, x_m^\dagger\} - (g_{m,k}\{a_k^\dagger, a_k\} + g_{m,k'}\{a_k^\dagger a_{k'} + a_k a_{k'}^\dagger\})[\![x_m, x_m^\dagger]\!]\big\}, \tag{B10}$$

$$[\![V_1, X_2]\!] = \lambda_{m,k}^+\big\{g_{m',k}(x_1 x_2 + x_1^\dagger x_2^\dagger) + g_{m,k}\{x_m^2 + x_m^{\dagger 2}\} + (g_{m,k}\{a_k^{+2} + a_k^{-2}\} + g_{m,k'}\{a_k^\dagger a_{k'} + a_k a_{k'}^\dagger\})[\![x_m, x_m^\dagger]\!]\big\}, \tag{B11}$$

$$[\![V_2, X_1]\!] = -\lambda_{m,k}^-\big\{g_{m',k}(x_1 x_2 + x_1^\dagger x_2^\dagger) + g_{m,k}\{x_m^2 + x_m^{\dagger 2}\} - (g_{m,k}\{a_k^{+2} + a_k^{-2}\} + g_{m,k'}\{a_k^\dagger a_{k'} + a_k a_{k'}^\dagger\})[\![x_m, x_m^\dagger]\!]\big\}, \tag{B12}$$

$$[\![V_2, X_2]\!] = \lambda_{m,k}^+\{g_{m',k}(x_1^\dagger x_2 + x_1 x_2^\dagger) + g_{m,k}\{x_m, x_m^\dagger\} + (g_{m,k}\{a_k^\dagger, a_k\} + g_{m,k'}\{a_k^\dagger a_{k'} + a_k a_{k'}^\dagger\})[\![x_m, x_m^\dagger]\!]\}. \tag{B13}$$

As before, we have omitted the summation symbol in the above formulas for simplicity of notation. The component-coupler interaction can be eliminated to the second-order accuracy if

$$\lambda_{m,k}^- = -\frac{g_{m,n}}{(\Delta_{m,n} - 2g_k)}, \; \lambda_{m,k}^+ = -\frac{g_{m,n}}{(\Sigma_{m,n} + 2g_k)} \tag{B14}$$

or

$$\lambda_{m,k}^-\Delta_{m,n} + 2(\lambda_{m,k}^+ - \lambda_{m,k}^-)g_k = -g_{m,n}, \; \lambda_{m,k}^+\Sigma_{m,n} + 2(\lambda_{m,k}^+ - \lambda_{m,k}^-)g_k = -g_{m,n}, \tag{B15}$$

which gives the following effective Hamiltonian:

$$\tilde{H} = \omega_m x_m^\dagger x_m + (\omega_c + 2g_k)a_k^\dagger a_k + \underline{g_k\left(a_k^{\dagger 2} + a_k^2\right)}$$
$$+ \frac{1}{2}(\lambda_{m,k}^+ - \lambda_{m,k}^-)g_{m',k}(x_1 + x_1^\dagger)(x_2 + x_2^\dagger) + \frac{1}{2}(\lambda_{m,k}^+ - \lambda_{m,k}^-)g_{m,k}(x_m + x_m^\dagger)^2$$
$$+ \frac{1}{2}(\lambda_{m,k}^+ + \lambda_{m,k}^-)g_{m,k}(a_k + a_k^\dagger)^2[\![x_m, x_m^\dagger]\!] + \frac{1}{2}(\lambda_{m,k}^+ + \lambda_{m,k}^-)g_{m,k'}(a_k^\dagger + a_k)(a_{k'}^\dagger + a_{k'})[\![x_m, x_m^\dagger]\!]. \tag{B16}$$

Here the underlined term exists only for an Ising-type interaction.

[1] A. O. Niskanen, K. Harrabi, F. Yoshihara, Y. Nakamura, S. Lloyd, and J. S. Tsai, Quantum coherent tunable coupling of superconducting qubits, Science **316**, 723 (2007).

[2] J. M. Chow, A. D. Córcoles, J. M. Gambetta, C. Rigetti, B. R. Johnson, J. A. Smolin, J. R. Rozen, G. A. Keefe, M. B. Rothwell, M. B. Ketchen, and M. Steffen, Simple all-Microwave Entangling Gate for Fixed-Frequency Superconducting Qubits, Phys. Rev. Lett. **107**, 080502 (2011).

[3] D. C. McKay, S. Filipp, A. Mezzacapo, E. Magesan, J. M. Chow, and J. M. Gambetta, Universal Gate for Fixed-Frequency Qubits via a Tunable Bus, Phys. Rev. Appl. **6**, 064007 (2016).

[4] S. A. Caldwell, N. Didier, C. A. Ryan, E. A. Sete, A. Hudson, P. Karalekas, R. Manenti, M. P. da Silva, R. Sinclair, E. Acala, N. Alidoust, J. Angeles, A. Bestwick, M. Block, B. Bloom, A. Bradley, C. Bui, L. Capelluto, R. Chilcott, J. Cordova *et al.*, Parametrically Activated Entangling Gates Using Transmon Qubits, Phys. Rev. Appl. **10**, 034050 (2018).

[5] F. Arute, K. Arya, R. Babbush, D. Bacon, J. C. Bardin, R. Barends, R. Biswas, S. Boixo, F. G. S. L. Brandao, D. A. Buell, B. Burkett, Y. Chen, Z. Chen, B. Chiaro, R. Collins, W. Courtney, A. Dunsworth, E. Farhi, B. Foxen, A. Fowler *et al.*, Quantum supremacy using a programmable superconducting processor, Nature (London) **574**, 505 (2019).

[6] B. Foxen, C. Neill, A. Dunsworth, P. Roushan, B. Chiaro, A. Megrant, J. Kelly, Z. Chen, K. Satzinger, R. Barends, F. Arute, K. Arya, R. Babbush, D. Bacon, J. C. Bardin, S. Boixo, D. Buell, B. Burkett, Y. Chen, R. Collins *et al.*, Demonstrating a Continuous Set of two-Qubit Gates for Near-Term Quantum Algorithms, Phys. Rev. Lett. **125**, 120504 (2020).

[7] Y. Xu, J. Chu, J. Yuan, J. Qiu, Y. Zhou, L. Zhang, X. Tan, Y. Yu, S. Liu, J. Li, F. Yan, and D. Yu, High-Fidelity, High-Scalability Two-Qubit Gate Scheme for Superconducting Qubits, Phys. Rev. Lett. **125**, 240503 (2020).

[8] A. Bengtsson, P. Vikstål, C. Warren, M. Svensson, X. Gu, A. F. Kockum, P. Krantz, C. Križan, D. Shiri, I.-M. Svensson, G. Tancredi, G. Johansson, P. Delsing, G. Ferrini, and J. Bylander, Improved Success Probability with Greater Circuit Depth for the Quantum Approximate Optimization Algorithm, Phys. Rev. Appl. **14**, 034010 (2020).

[9] M. C. Collodo, J. Herrmann, N. Lacroix, C. K. Andersen, A. Remm, S. Lazar, J.-C. Besse, T. Walter, A. Wallraff, and C. Eichler, Implementation of Conditional Phase Gates Based on Tunable *zz* Interactions, Phys. Rev. Lett. **125**, 240502 (2020).

[10] A. Blais, A. Maassen van den Brink, and A. M. Zagoskin, Tunable Coupling of Superconducting Qubits, Phys. Rev. Lett. **90**, 127901 (2003).

[11] J. M. Gambetta, A. A. Houck, and A. Blais, Superconducting Qubit with Purcell Protection and Tunable Coupling, Phys. Rev. Lett. **106**, 030502 (2011).

[12] R. C. Bialczak, M. Ansmann, M. Hofheinz, M. Lenander, E. Lucero, M. Neeley, A. D. O'Connell, D. Sank, H. Wang, M. Weides, J. Wenner, T. Yamamoto, A. N. Cleland, and J. M. Martinis, Fast tunable Coupler for Superconducting Qubits, Phys. Rev. Lett. **106**, 060501 (2011).

[13] Y. Chen, C. Neill, P. Roushan, N. Leung, M. Fang, R. Barends, J. Kelly, B. Campbell, Z. Chen, B. Chiaro, A. Dunsworth, E. Jeffrey, A. Megrant, J. Y. Mutus, P. J. J. O'Malley, C. M. Quintana, D. Sank, A. Vainsencher, J. Wenner, T. C. White *et al.*, Qubit Architecture with High Coherence and Fast Tunable Coupling, Phys. Rev. Lett. **113**, 220502 (2014).

[14] M. R. Geller, E. Donate, Y. Chen, M. T. Fang, N. Leung, C. Neill, P. Roushan, and J. M. Martinis, Tunable coupler for superconducting Xmon qubits: Perturbative nonlinear model, Phys. Rev. A **92**, 012320 (2015).

[15] C. P. Sun, L. F. Wei, Y.-x. Liu, and F. Nori, Quantum transducers: Integrating transmission lines and nanomechanical resonators via charge qubits, Phys. Rev. A **73**, 022318 (2006).

[16] M. Mariantoni, F. Deppe, A. Marx, R. Gross, F. K. Wilhelm, and E. Solano, Two-resonator circuit quantum electrodynamics: A superconducting quantum switch, Phys. Rev. B **78**, 104508 (2008).

[17] S. J. Srinivasan, A. J. Hoffman, J. M. Gambetta, and A. A. Houck, Tunable Coupling in Circuit Quantum Electrodynamics Using a Superconducting Charge Qubit with a *v*-Shaped Energy Level Diagram, Phys. Rev. Lett. **106**, 083601 (2011).

[18] A. Baust, E. Hoffmann, M. Haeberlein, M. J. Schwarz, P. Eder, J. Goetz, F. Wulschner, E. Xie, L. Zhong, F. Quijandría, B. Peropadre, D. Zueco, J.-J. García Ripoll, E. Solano, K. Fedorov, E. P. Menzel, F. Deppe, A. Marx, and R. Gross, Tunable and switchable coupling between two superconducting resonators, Phys. Rev. B **91**, 014515 (2015).

[19] F. Yan, P. Krantz, Y. Sung, M. Kjaergaard, D. L. Campbell, T. P. Orlando, S. Gustavsson, and W. D. Oliver, Tunable Coupling Scheme for Implementing High-Fidelity two-Qubit Gates, Phys. Rev. Appl. **10**, 054062 (2018).

[20] P. Mundada, G. Zhang, T. Hazard, and A. Houck, Suppression of Qubit Crosstalk in a Tunable Coupling Superconducting Circuit, Phys. Rev. Appl. **12**, 054023 (2019).

[21] X. Li, T. Cai, H. Yan, Z. Wang, X. Pan, Y. Ma, W. Cai, J. Han, Z. Hua, X. Han, Y. Wu, H. Zhang, H. Wang, Y. Song, L. Duan, and L. Sun, Tunable Coupler for Realizing a Controlled-Phase Gate

with Dynamically Decoupled Regime in a Superconducting Circuit, Phys. Rev. Appl. **14**, 024070 (2020).

[22] X. Y. Han, T. Q. Cai, X. G. Li, Y. K. Wu, Y. W. Ma, Y. L. Ma, J. H. Wang, H. Y. Zhang, Y. P. Song, and L. M. Duan, Error analysis in suppression of unwanted qubit interactions for a parametric gate in a tunable superconducting circuit, Phys. Rev. A **102**, 022619 (2020).

[23] R. H. Dicke, Coherence in spontaneous radiation processes, Phys. Rev. **93**, 99 (1954).

[24] Q.-M. Chen, Y.-x. Liu, L. Sun, and R.-B. Wu, Tuning the coupling between superconducting resonators with collective qubits, Phys. Rev. A **98**, 042328 (2018).

[25] M. O. Scully, Single Photon Subradiance: Quantum Control of spontaneous Emission and Ultrafast Readout, Phys. Rev. Lett. **115**, 243602 (2015).

[26] J. M. Fink, R. Bianchetti, M. Baur, M. Göppl, L. Steffen, S. Filipp, P. J. Leek, A. Blais, and A. Wallraff, Dressed Collective Qubit States and the Tavis-Cummings Model in Circuit QED, Phys. Rev. Lett. **103**, 083601 (2009).

[27] S. Filipp, A. F. van Loo, M. Baur, L. Steffen, and A. Wallraff, Preparation of subradiant states using local qubit control in circuit QED, Phys. Rev. A **84**, 061805(R) (2011).

[28] S. Filipp, M. Göppl, J. M. Fink, M. Baur, R. Bianchetti, L. Steffen, and A. Wallraff, Multimode mediated qubit-qubit coupling and dark-state symmetries in circuit quantum electrodynamics, Phys. Rev. A **83**, 063827 (2011).

[29] M. Delanty, S. Rebić, and J. Twamley, Superradiance and phase multistability in circuit quantum electrodynamics, New J. Phys. **13**, 053032 (2011).

[30] A. F. van Loo, A. Fedorov, K. Lalumiére, B. C. Sanders, A. Blais, and A. Wallraff, Photon-mediated interactions between distant artificial atoms, Science **342**, 1494 (2013).

[31] J. Mlynek, A. Abdumalikov, C. Eichler, and A. Wallraff, Observation of Dicke superradiance for two artificial atoms in a cavity with high decay rate, Nat. Commun. **5**, 5186 (2014).

[32] R. Ma, B. Saxberg, C. Owens, N. Leung, Y. Lu, J. Simon, and D. I. Schuster, A dissipatively stabilized Mott insulator of photons, Nature (London) **566**, 51 (2019).

[33] C. Song, K. Xu, H. Li, Y.-R. Zhang, X. Zhang, W. Liu, Q. Guo, Z. Wang, W. Ren, J. Hao, H. Feng, H. Fan, D. Zheng, D.-W. Wang, H. Wang, and S.-Y. Zhu, Generation of multicomponent atomic Schrödinger cat states of up to 20 qubits, Science **365**, 574 (2019).

[34] Y. Ye, Z.-Y. Ge, Y. Wu, S. Wang, M. Gong, Y.-R. Zhang, Q. Zhu, R. Yang, S. Li, F. Liang, J. Lin, Y. Xu, C. Guo, L. Sun, C. Cheng, N. Ma, Z. Y. Meng, H. Deng, H. Rong, C.-Y. Lu *et al.*, Propagation and Localization of Collective Excitations on a 24-Qubit Superconducting Processor, Phys. Rev. Lett. **123**, 050502 (2019).

[35] Z. Yan, Y.-R. Zhang, M. Gong, Y. Wu, Y. Zheng, S. Li, C. Wang, F. Liang, J. Lin, Y. Xu, C. Guo, L. Sun, C.-Z. Peng, K. Xia, H. Deng, H. Rong, J. Q. You, F. Nori, H. Fan, X. Zhu *et al.*, Strongly correlated quantum walks with a 12-qubit superconducting processor, Science **364**, 753 (2019).

[36] Z. Wang, H. Li, W. Feng, X. Song, C. Song, W. Liu, Q. Guo, X. Zhang, H. Dong, D. Zheng, H. Wang, and D.-W. Wang, Controllable Switching Between Superradiant and Subradiant States in a 10-Qubit Superconducting Circuit, Phys. Rev. Lett. **124**, 013601 (2020).

[37] M. Gong, S. Wang, C. Zha, M.-C. Chen, H.-L. Huang, Y. Wu, Q. Zhu, Y. Zhao, S. Li, S. Guo, H. Qian, Y. Ye, F. Chen, C. Ying, J. Yu, D. Fan, D. Wu, H. Su, H. Deng, H. Rong *et al.*, Quantum walks on a programmable two-dimensional 62-qubit superconducting processor, Science **372**, 948 (2021).

[38] A. Blais, R.-S. Huang, A. Wallraff, S. M. Girvin, and R. J. Schoelkopf, Cavity quantum electrodynamics for superconducting electrical circuits: An architecture for quantum computation, Phys. Rev. A **69**, 062320 (2004).

[39] M. Tavis and F. W. Cummings, Exact solution for an *N*-molecule–radiation-field Hamiltonian, Phys. Rev. **170**, 379 (1968).

[40] M. Tavis and F. W. Cummings, Approximate solutions for an *N*-molecule-radiation-field Hamiltonian, Phys. Rev. **188**, 692 (1969).

[41] C. E. López, H. Christ, J. C. Retamal, and E. Solano, Effective quantum dynamics of interacting systems with inhomogeneous coupling, Phys. Rev. A **75**, 033818 (2007).

[42] M. Forsch, R. Stockill, A. Wallucks, I. Marinković, C. Gärtner, R. A. Norte, F. van Otten, A. Fiore, K. Srinivasan, and S. Gröblacher, Microwave-to-optics conversion using a mechanical oscillator in its quantum ground state, Nat. Phys. **16**, 69 (2019).

[43] J. Schwinger, On Angular Momentum, techreport NYO-3071 (Nuclear Development Associates, Inc., 1952).

[44] J. J. Sakurai, *Modern Quantum Mechanics*, revised ed. (Pearson, New York, 1994).

[45] H. J. Carmichael, *Statistical Methods in Quantum Optics 1: Master Equations and Fokker-Planck Equations* (Springer, New York, 1999).

[46] M. Mariantoni, E. P. Menzel, F. Deppe, M. A. Araque Caballero, A. Baust, T. Niemczyk, E. Hoffmann, E. Solano, A. Marx, and R. Gross, Planck Spectroscopy and Quantum Noise of Microwave Beam Splitters, Phys. Rev. Lett. **105**, 133601 (2010).

[47] E. P. Menzel, F. Deppe, M. Mariantoni, M. A. Araque Caballero, A. Baust, T. Niemczyk, E. Hoffmann, A. Marx, E. Solano, and R. Gross, Dual-Path State Reconstruction Scheme for Propagating Quantum Microwaves and Detector Noise Tomography, Phys. Rev. Lett. **105**, 100401 (2010).

[48] E. P. Menzel, R. Di Candia, F. Deppe, P. Eder, L. Zhong, M. Ihmig, M. Haeberlein, A. Baust, E. Hoffmann, D. Ballester, K. Inomata, T. Yamamoto, Y. Nakamura, E. Solano, A. Marx, and R. Gross, Path Entanglement of Continuous-Variable Quantum Microwaves, Phys. Rev. Lett. **109**, 250502 (2012).

[49] K. G. Fedorov, L. Zhong, S. Pogorzalek, P. Eder, M. Fischer, J. Goetz, E. Xie, F. Wulschner, K. Inomata, T. Yamamoto, Y. Nakamura, R. Di Candia, U. Las Heras, M. Sanz, E. Solano, E. P. Menzel, F. Deppe, A. Marx, and R. Gross, Displacement of Propagating Squeezed Microwave States, Phys. Rev. Lett. **117**, 020502 (2016).

[50] E. T. Jaynes and F. W. Cummings, Comparison of quantum and semiclassical radiation theories with application to the beam maser, Proc. IEEE **51**, 89 (1963).

[51] J. Katriel, A. I. Solomon, G. D'Ariano, and M. Rasetti, Multiboson Holstein-Primakoff squeezed states for SU(2) and SU(1,1), Phys. Rev. D **34**, 2332 (1986).

[52] R. K. Bullough, Photon, quantum and collective, effects from Rydberg atoms in cavities, Hyperfine Interact. **37**, 71 (1987).

[53] R. K. Bullough, G. S. Agarwal, B. M. Garraway, S. S. Hassan, G. P. Hildred, S. V. Lawande, N. Nayak, R. R. Puri, B. V. Thompson, J. Timonen, and M. R. B. Wahiddin, Giant quantum oscillators from Rydberg atoms: Atomic coherent states and their squeezing from Rydberg atoms, in *Squeezed and Nonclassical Light*, edited by P. Tombesi and E. R. Pike (Springer US, Boston, 1989), pp. 81–106.

[54] C. Emary and T. Brandes, Quantum Chaos Triggered by Precursors of a Quantum Phase Transition: The Dicke Model, Phys. Rev. Lett. **90**, 044101 (2003).

[55] C. Emary and T. Brandes, Chaos and the quantum phase transition in the Dicke model, Phys. Rev. E **67**, 066203 (2003).

[56] P. Karbach and J. Stolze, Spin chains as perfect quantum state mirrors, Phys. Rev. A **72**, 030301(R) (2005).

[57] A. Wójcik, T. Łuczak, P. Kurzyński, A. Grudka, T. Gdala, and M. Bednarska, Unmodulated spin chains as universal quantum wires, Phys. Rev. A **72**, 034303 (2005).

[58] A. Wójcik, T. Łuczak, P. Kurzyński, A. Grudka, T. Gdala, and M. Bednarska, Multiuser quantum communication networks, Phys. Rev. A **75**, 022330 (2007).

[59] A. Gratsea, G. M. Nikolopoulos, and P. Lambropoulos, Photon-assisted quantum state transfer and entanglement generation in spin chains, Phys. Rev. A **98**, 012304 (2018).

[60] A. A. Clerk, M. H. Devoret, S. M. Girvin, F. Marquardt, and R. J. Schoelkopf, Introduction to quantum noise, measurement, and amplification, Rev. Mod. Phys. **82**, 1155 (2010).

[61] J. L. G. Muñoz and F. Delgado, QUANTUM: A Wolfram Mathematica add-on for Dirac bra-ket notation, non-commutative algebra, and simulation of quantum computing circuits, J. Phys.: Conf. Ser. **698**, 012019 (2016).

[62] The codes for deriving the effective Hamiltonian are available at www.notebookarchive.org/2021-07-duvj15v.

[63] J. Johansson, P. Nation, and F. Nori, QuTiP 2: A Python framework for the dynamics of open quantum systems, Comput. Phys. Commun. **184**, 1234 (2013).

[64] D. Zueco, G. M. Reuther, S. Kohler, and P. Hänggi, Qubit-oscillator dynamics in the dispersive regime: Analytical theory beyond the rotating-wave approximation, Phys. Rev. A **80**, 033846 (2009).